Time-Optimal Frictionless Atom Cooling in Harmonic Traps

Dionisis Stefanatos, Heinz Schaettler, and Jr-Shin Li

Abstract—**Frictionless atom cooling in harmonic traps is formulated as a time-optimal control problem and a synthesis of optimal controlled trajectories is obtained. This work has already been used to determine the minimum time for transition between two thermal states and to show the emergence of the third law of classical thermodynamics from quantum thermodynamics. It can also find application in the fast adiabatic-like expansion of Bose-Einstein condensates, with possible applications in atom interferometry. This paper is based on our recently published article in *SIAM J. Control Optim.* [1].**

Index Terms—Quantum control, time-optimal control, atom cooling, quantum thermodynamics

I. INTRODUCTION

During the last decades, a wealth of analytical and numerical tools from control theory and optimization have been successfully employed to analyze and control the performance of quantum mechanical systems, advancing quantum technology in areas as diverse as physical chemistry, metrology, and quantum information processing [2]. Although measurement-based feedback control [3] and the promising coherent feedback control [4] have gained considerable attention, open-loop control has been proven quite effective. Analytical solutions for optimal control problems defined on low-dimensional quantum systems have been derived, leading to novel pulse sequences with unexpected gains compared with those traditionally used [5]–[10], while numerical optimization methods, based on gradient algorithms or direct approaches, have been used to address more complex tasks and to minimize the effect of the ubiquitous experimental imperfections [11]–[13].

At the heart of modern quantum technology lies the efficient cooling of trapped atoms, since it has created the ultimate physical systems thus far for precision spectroscopy, frequency standards, and even tests of fundamental physics [14], as well as candidate systems for quantum information processing [15]. In the present article we study a time-optimal control problem related to the frictionless cooling of atoms trapped in a time-dependent harmonic potential. Frictionless atom cooling in a harmonic trapping potential is defined as the problem of changing the harmonic frequency of the trap to some lower final value, while keeping the populations of the initial and final levels invariant, thus without generating friction and heating. Conventionally, an adiabatic process is used where the frequency is changed slowly and the system follows the instantaneous eigenvalues and eigenstates of the time-dependent Hamiltonian. The drawback of this method is

the long necessary times which may render it impractical. A way to bypass this problem is to use the theory of the time-dependent quantum harmonic oscillator [16] to prepare the same final states and energies as with the adiabatic process at a given final time, without necessarily following the instantaneous eigenstates at each moment. Achieving this goal in minimum time has many important potential applications. For example, it can be used to reach extremely low temperatures inaccessible by standard cooling techniques [17] and to reduce the velocity dispersion and collisional shifts for spectroscopy and atomic clocks [18]. It is also closely related to the problem of moving in minimum time a system between two thermal states [19].

It was initially proved that minimum transfer time for the aforementioned problem can be achieved with "bang-bang" real frequency controls [19]. Later, it was shown that when the restriction for real frequencies is relaxed, allowing the trap to become an expulsive parabolic potential at some time intervals, shorter transfer times can be obtained, leading to a "shortcut to adiabaticity" [20]. In our recent work [21], we formulated frictionless atom cooling as a minimum-time optimal control problem, permitting the frequency to take real and imaginary values in specified ranges. We showed that the optimal solution has again a "bang-bang" form and used this fact to obtain estimates of the minimum transfer times for various numbers of switchings. In the present article we complete our previous work by fully solving the corresponding time-optimal control problem and obtaining the optimal synthesis. The results presented here have already been used to determine the minimum time for transition between two thermal states [22] and to show the emergence of the third law of classical thermodynamics from quantum thermodynamics [23], as highlighted in the conclusion.

II. FORMULATION OF THE PROBLEM IN TERMS OF OPTIMAL CONTROL

The evolution of the wavefunction $\psi(t, x)$ of a particle in a one-dimensional parabolic trapping potential with time-varying frequency $\omega(t)$ is given by the Schrödinger equation

$$i\hbar \frac{\partial \psi}{\partial t} = \left[-\frac{\hbar^2}{2m} \frac{\partial^2}{\partial x^2} + \frac{m\omega^2(t)}{2} x^2 \right] \psi, \quad (1)$$

where m is the particle mass and $\hbar$ is Planck's constant; $x \in \mathbb{R}$ and ψ is a square-integrable function on the real line. When $\omega(t)$ is *constant*, the above equation can be solved by separation of variables and the solution is $\psi(t, x) = \sum_{n=0}^{\infty} c_n e^{-iE_n^\omega t/\hbar} \Psi_n^\omega(x)$, where E_n^ω are the eigenvalues and $\Psi_n^\omega(x)$ are the eigenfunctions of the quantum harmonic oscillator [24]. The coefficients c_n can be found from the initial condition $c_n = \int_{-\infty}^{\infty} \psi(0, x) \Psi_n^\omega(x) dx$.
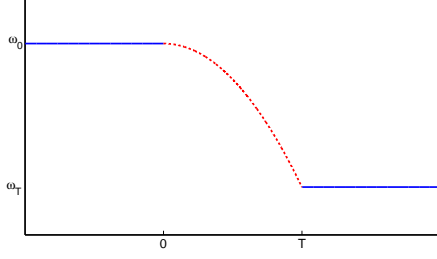
Fig. 1. Time evolution of the harmonic trap frequency.

Consider now the case shown in Fig. 1, where $\omega(t) = \omega_0$ for $t \leq 0$ and $\omega(t) = \omega_T < \omega_0$ for $t \geq T$. This corresponds to a temperature reduction by a factor ω_T/ω_0, if the initial and final states are canonical [20]. For frictionless cooling, the path $\omega(t)$ between these two values should be chosen so that the populations of all the oscillator levels $n = 0, 1, 2, \ldots$ for $t \geq T$ are equal to the ones at $t = 0$. In other words, if

$$\psi(0, x) = \sum_{n=0}^{\infty} c_n(0) \Psi_n^{\omega_0}(x),$$

and

$$\psi(t, x) = \sum_{n=0}^{\infty} c_n(t) \Psi_n^{\omega_T}(x), \ t \geq T,$$

then frictionless cooling is achieved when

$$|c_n(t)|^2 = |c_n(0)|^2, \ t \geq T, n = 0, 1, 2, \ldots \quad (2)$$

Among all the paths $\omega(t)$ that result in (2), we would like to find one that achieves frictionless cooling in minimum time T. In the following we provide a sufficient condition on $\omega(t)$ for frictionless cooling and we use it to formulate the corresponding time-optimal control problem.

Proposition 1: [1] If $\omega(t)$, with $\omega(0) = \omega_0$ and $\omega(t) = \omega(T) = \omega_T$ for $t \geq T$ is such that the Ermakov equation

$$\ddot{b}(t) + \omega^2(t) b(t) = \frac{\omega_0^2}{b^3(t)} \quad (3)$$

has a solution $b(t)$ with $b(0) = 1, \dot{b}(0) = 0$ and $b(t) = b(T) = (\omega_0/\omega_T)^{1/2}, t \geq T$, then condition (2) for frictionless cooling is satisfied.

If we set

$$x_1 = b, \ x_2 = \frac{\dot{b}}{\omega_0}, \ u(t) = \frac{\omega^2(t)}{\omega_0^2}, \quad (4)$$

and rescale time according to $t_{\text{new}} = \omega_0 t_{\text{old}}$, we obtain the following system of first order differential equations, equivalent to the Ermakov equation

$$\dot{x}_1 = x_2, \quad (5)$$

$$\dot{x}_2 = -u x_1 + \frac{1}{x_1^3}. \quad (6)$$

By incorporating the boundary conditions and possible restrictions on $\omega(t)$ due, for example, to experimental limitations, and setting $\gamma = (\omega_0/\omega_T)^{1/2} > 1$, we obtain the following time-optimal problem for frictionless cooling

problem 1: Find $-u_1 \leq u(t) \leq u_2$ with $u(0) = 1, u(T) = 1/\gamma^4$ such that starting from $(x_1(0), x_2(0)) = (1, 0)$, the above system reaches the final point $(x_1(T), x_2(T)) = (\gamma, 0), \gamma > 1$, in minimum time T.

The boundary conditions on the state variables (x_1, x_2) are equivalent to those for $b, \dot{b}$, while the boundary conditions on the control variable u are equivalent to those for ω, so the requirements of Proposition 1 are satisfied. Parameters $u_1, u_2 > 0$ define the allowable values of $u(t)$ and it is $u_2 \geq u(0) = 1$. Note that the possibility $\omega^2(t) < 0$ (expulsive parabolic potential) for some time intervals is permitted [20]. It is natural to consider that also $u_1 \geq 1$, i.e. we can at least achieve the negative potential $V(x) = -m\omega_0^2 x^2/2$. Finally observe that the above system describes the one-dimensional Newtonian motion of a unit-mass particle, with position coordinate x_1 and velocity x_2. The acceleration (force) acting on the particle is $-ux_1 + 1/x_1^3$. This point of view can provide useful intuition about the time-optimal solution, as we will see later.

In the next section we solve the following optimal control problem

problem 2: Find $-u_1 \leq u(t) \leq u_2$, with $u_1, u_2 \geq 1$, such that starting from $(x_1(0), x_2(0)) = (1, 0)$, the system above reaches the final point $(x_1(T), x_2(T)) = (\gamma, 0), \gamma > 1$, in minimum time T.

In both problems the class of admissible controls formally are Lebesgue measurable functions that take values in the control set $[-u_1, u_2]$ almost everywhere. However, as we shall see, optimal controls are piecewise continuous, in fact bang-bang. The optimal control found for problem 2 is also optimal for problem 1, with the addition of instantaneous jumps at the initial and final points, so that the boundary conditions $u(0) = 1$ and $u(T) = 1/\gamma^4$ are satisfied. Note that in connection with Fig. 1, a natural way to think about these conditions is that $u(t) = 1$ for $t \leq 0$ and $u(t) = 1/\gamma^4$ for $t \geq T$; in the interval $(0, T)$ we pick the control that achieves the desired transfer in minimum time.

III. OPTIMAL SOLUTION

The system described by (5), (6) can be expressed in compact form as

$$\dot{x} = f(x) + u g(x), \quad (7)$$

where the vector fields are given by

$$f = \begin{pmatrix} x_2 \\ 1/x_1^3 \end{pmatrix}, \ g = \begin{pmatrix} 0 \\ -x_1 \end{pmatrix} \quad (8)$$

and $x \in \mathcal{D} = \{(x_1, x_2) \in \mathbb{R}^2 : x_1 > 0\}$ and $u \in U = [-u_1, u_2]$. Admissible controls are Lebesgue measurable functions that take values in the control set U. Given an admissible control u defined over an interval $[0, T]$, the solution x of the system (7) corresponding to the control u is called the corresponding trajectory and we call the pair (x, u) a controlled trajectory. Note that the domain $\mathcal{D}$ is invariant in the sense that trajectories cannot leave $\mathcal{D}$. Starting with any positive initial condition $x_1(0) > 0$, and using any admissible control u, as $x_1 \to 0^+$, the "repulsive force" $1/x_1^3$ leads to

an increase in x_1 that will keep x_1 positive (as long as the solutions exist).

For a constant λ_0 and a row vector $\lambda = (\lambda_1, \lambda_2) \in \left(\mathbb{R}^2\right)^*$ define the control Hamiltonian as

$$H = H(\lambda_0, \lambda, x, u) = \lambda_0 + \langle \lambda, f(x) + ug(x)\rangle.$$

Pontryagin's Maximum Principle [25] provides the following necessary conditions for optimality:

Theorem 1 (Maximum principle): [25] Let $(x_*(t), u_*(t))$ be a time-optimal controlled trajectory that transfers the initial condition $x(0) = x_0$ into the terminal state $x(T) = x_T$. Then it is a necessary condition for optimality that there exists a constant $\lambda_0 \leq 0$ and nonzero, absolutely continuous row vector function $\lambda(t)$ such that:

1) λ satisfies the so-called adjoint equation

$$\dot{\lambda}(t) = -\frac{\partial H}{\partial x}(\lambda_0, \lambda(t), x_*(t), u_*(t))$$

2) For $0 \leq t \leq T$ the function $u \mapsto H(\lambda_0, \lambda(t), x_*(t), u)$ attains its maximum over the control set U at $u = u_*(t)$.
3) $H(\lambda_0, \lambda(t), x_*(t), u_*(t)) \equiv 0$.

We call a controlled trajectory (x, u) for which there exist multipliers λ_0 and $\lambda(t)$ such that these conditions are satisfied an extremal. Extremals for which $\lambda_0 = 0$ are called abnormal. If $\lambda_0 < 0$, then without loss of generality we may rescale the λ's and set $\lambda_0 = -1$. Such an extremal is called normal.

For the system (5), (6) we have

$$H(\lambda_0, \lambda, x, u) = \lambda_0 + \lambda_1 x_2 + \lambda_2 \left(\frac{1}{x_1^3} - x_1 u\right), \quad (9)$$

and thus

$$\dot{\lambda} = -\lambda \begin{pmatrix} 0 & 1 \\ -(u + 3/x_1^4) & 0 \end{pmatrix} = -\lambda A \quad (10)$$

Observe that H is a linear function of the bounded control variable u. The coefficient at u in H is $-\lambda_2 x_1$ and, since $x_1 > 0$, its sign is determined by $\Phi = -\lambda_2$, the so-called *switching function*. According to the maximum principle, point 2 above, the optimal control is given by $u = -u_1$ if $\Phi < 0$ and by $u = u_2$ if $\Phi > 0$. The maximum principle provides a priori no information about the control at times t when the switching function Φ vanishes. However, if $\Phi(t) = 0$ and $\dot{\Phi}(t) \neq 0$, then at time t the control switches between its boundary values and we call this a bang-bang switch. If Φ were to vanish identically over some open time interval I the corresponding control is called *singular*.

Proposition 2: For Problem 2 optimal controls are bang-bang.

Proof: Whenever the switching function $\Phi(t) = -\lambda_2(t)$ vanishes at some time t, then it follows from the non-triviality of the multiplier $\lambda(t)$ that its derivative $\dot{\Phi}(t) = -\dot{\lambda}_2(t) = \lambda_1(t)$ is non-zero. Hence the switching function changes sign and there is a bang-bang switch at time t. ∎

Definition 1: We denote the vector fields corresponding to the constant bang controls $-u_1$ and u_2 by $X = f - u_1 g$ and $Y = f + u_2 g$, respectively, and call the trajectories corresponding to the constant controls $u \equiv -u_1$ and $u \equiv u_2$ X- and Y-trajectories. A concatenation of an X-trajectory followed by a Y-trajectory is denoted by XY while the concatenation in the inverse order is denoted by YX.

In this paper we establish the precise concatenation sequences for optimal controls and in particular calculate the times between switchings explicitly.

Proposition 3: All the extremals are normal.

Proof: If (x, u) is an abnormal extremal trajectory that has a switching at time t, then, since $\lambda_2(t) = 0$, it follows from $H = 0$ that we must have $x_2(t) = 0$. The starting point is $(1, 0)$ and suppose that $u = -u_1$ initially. From (6) it is $\dot{x}_2 > 0$ so $x_2 > 0$ and a switching at a point with $x_2(t) > 0$, not allowed for an abnormal extremal, is necessary in order to reach the target point $(\gamma, 0)$. If $u = u_2$ initially, then $\dot{x}_2(0) = 1 - u_2 < 0$ and $x_2 < 0$ for some time interval. During this time it is $\dot{x}_1 < 0$ and consequently $x_1 < 1 < \gamma$. A switching is necessary, which takes place on the x_1-axis for an abnormal extremal. The control changes to $u = -u_1$ and the situation is as before, where one more switching is necessary at a point with $x_2(t) > 0$, forbidden for abnormal extremals. Thus, there are no abnormal extremals in the optimal solutions. ∎

For normal extremals we can set $\lambda_0 = -1$. Then, $H = 0$ implies that for any switching time t we must have $\lambda_1(t)x_2(t) = 1$. For an XY junction we have $\dot{\Phi}(t) = \lambda_1(t) > 0$ and thus necessarily $x_2(t) > 0$ and analogously optimal YX junctions need to lie in $\{x_2 < 0\}$. We now develop the precise structure of the switchings in a series of Lemmas.

Lemma 1 (First integrals): A first integral of the motion along the X-trajectory passing through $(\alpha, 0)$ is

$$x_2^2 - u_1 x_1^2 + \frac{1}{x_1^2} = -u_1 \alpha^2 + \frac{1}{\alpha^2}, \quad (11)$$

while a first integral of the motion along the Y-trajectory passing through $(\beta, 0)$ is

$$x_2^2 + u_2 x_1^2 + \frac{1}{x_1^2} = u_2 \beta^2 + \frac{1}{\beta^2}. \quad (12)$$

Proof: Use the system equations (5) and (6). ∎

Lemma 2 (Inter-switching time): Let $p = (x_1, x_2)$ be a switching point and τ denote the time to reach the next switching point q. If $\overrightarrow{pq}$ is a Y-trajectory, then

$$\sin(2\sqrt{u_2}\tau) = -\frac{2\sqrt{u_2}x_1 x_2}{x_2^2 + u_2 x_1^2}, \quad \cos(2\sqrt{u_2}\tau) = \frac{x_2^2 - u_2 x_1^2}{x_2^2 + u_2 x_1^2} \quad (13)$$

while, if $\overrightarrow{pq}$ is an X-trajectory, then

$$\sinh(2\sqrt{u_1}\tau) = -\frac{2\sqrt{u_1}x_1 x_2}{x_2^2 - u_1 x_1^2}, \quad \cosh(2\sqrt{u_1}\tau) = \frac{x_2^2 + u_1 x_1^2}{x_2^2 - u_1 x_1^2}. \quad (14)$$

Note that the inter-switching times depend only on the ratio x_2/x_1.

Proof: These formulas are obtained as an application of the concept of a "conjugate point" for bang-bang controls [26]. Without loss of generality assume that the trajectory passes through p at time 0 and is at q at time τ. Since p and q are switching points, the corresponding multipliers vanish against the control vector field g at those points, i.e., $\langle \lambda(0), g(p)\rangle = \langle \lambda(\tau), g(q)\rangle = 0$. We need to compute what the relation $\langle \lambda(\tau), g(q)\rangle = 0$ implies at time 0. In order to do so, we move the vector $g(q)$ along the Y-trajectory backward

from q to p. This is done by means of the solution $w(t)$ of the variational equation along the Y-trajectory with terminal condition $w(\tau) = g(q)$ at time τ. Recall that the variational equation along Y is the linear system $\dot{w} = Aw$ where A is given in (10). Symbolically, if we denote by $e^{tY}(p)$ the value of the Y-trajectory at time t that starts at the point p at time 0 and by $(e^{-tY})_*$ the backward evolution under the linear differential equation $\dot{w} = Aw$, then we can represent this solution in the form

$$w(0) = (e^{-\tau Y})_* w(\tau) = (e^{-\tau Y})_* g(q)$$
$$= (e^{-\tau Y})_* g(e^{\tau Y}(p)) = (e^{-\tau Y})_* \circ g \circ e^{\tau Y}(p).$$

Since the "adjoint equation" of the Maximum Principle is precisely the adjoint equation to the variational equation, it follows that the function $t \mapsto \langle \lambda(t), w(t) \rangle$ is constant along the Y-trajectory. Hence $\langle \lambda(\tau), g(q) \rangle = 0$ implies that

$$\langle \lambda(0), w(0) \rangle = \langle \lambda(0), (e^{-\tau Y})_* g(e^{\tau Y}(p)) \rangle = 0$$

as well. But the non-zero multiplier $\lambda(0)$ can only be orthogonal to both $g(p)$ and $w(0)$ if these vectors are parallel, $g(p) \| w(0) = (e^{-\tau Y})_* g(e^{\tau Y}(p))$. It is this relation that defines the switching time.

It remains to compute $w(0)$. For this we make use of the well-known relation [27]

$$(e^{-\tau Y})_* \circ g \circ e^{\tau Y} = e^{\tau \, adY}(g) \qquad (15)$$

where the operator adY is defined as $adY(g) = [Y, g]$, with $[,]$ denoting the Lie bracket of the vector fields Y and g. For our system, the Lie algebra $\mathcal{L}$ generated by the fields f and g actually is finite dimensional: we have

$$[f, g](x) = \begin{pmatrix} x_1 \\ -x_2 \end{pmatrix}$$

and the relations

$$[f, [f, g]] = 2f, \qquad [g, [f, g]] = -2g$$

can be directly verified. Using these relations and the analyticity of the system, $e^{t \, adY}(g)$ can be calculated in closed form from the expansion

$$e^{t \, adY}(g) = \sum_{n=0}^{\infty} \frac{t^n}{n!} \, ad^n Y(g), \qquad (16)$$

where, inductively, $ad^n Y(g) = [Y, ad^{n-1} Y(g)]$. It is not hard to show that for $n = 0, 1, 2, \ldots$, we have that

$$ad^{2n+1} Y(g) = (-4u_2)^n [f, g]$$

and

$$ad^{2n+2} Y(g) = 2(-4u_2)^n (f - u_2 g),$$

so that

$$e^{t \, adY}(g) = g + \sum_{n=0}^{\infty} \frac{t^{2n+1}}{(2n+1)!} (-4u_2)^n [f, g]$$
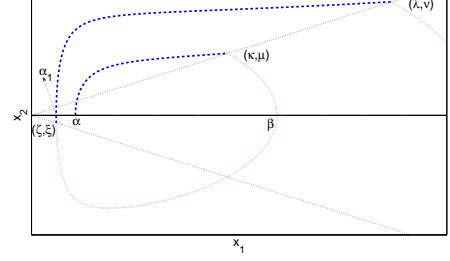$$+ \sum_{n=0}^{\infty} \frac{2t^{2n+2}}{(2n+2)!} (-4u_2)^n (f - u_2 g).$$

Fig. 2. Consecutive switching points lie on two opposite-slope lines through the origin. Blue dashed curves correspond to X-segments, red dotted curves to Y-segments.

By summing the series appropriately we obtain

$$e^{t \, adY}(g) = g + \frac{1}{2\sqrt{u_2}} \sin(2\sqrt{u_2}t)[f, g]$$
$$+ \frac{1}{2u_2}[1 - \cos(2\sqrt{u_2}t)](f - u_2 g).$$

Hence the field $w(0) = (e^{-\tau Y})_* g(e^{\tau Y}(p))$ is parallel to $g(p) = (0, -x_1)^T$ if and only if

$$\sqrt{u_2} x_1 \sin(2\sqrt{u_2}\tau) + x_2 [1 - \cos(2\sqrt{u_2}\tau)] = 0.$$

Hence

$$\sin(2\sqrt{u_2}\tau) = -\frac{x_2}{\sqrt{u_2} x_1}[1 - \cos(2\sqrt{u_2}\tau)] \qquad (17)$$

from which (13) follows. Note that the solution $\cos(2\sqrt{u_2}\tau) = 1$ is rejected because it corresponds to $\tau = 0$ or $\tau = \pi/\sqrt{u_2}$, the latter being the period of the closed trajectory.

Working analogously for an X-trajectory we obtain (14). $\blacksquare$

Lemma 3 (Main technical point): The ratio of the coordinates of consecutive switching points has constant magnitude but alternating sign, while these points are not symmetric with respect to the x_1-axis.

Proof: Consider the trajectory shown in Fig. 2, with switching points $(\kappa, \mu), (\zeta, \xi)$ and (λ, ν). Starting from (κ, μ) and integrating the equations of motion (5) and (6) for the inter-switching time given in (13), we can find the coordinates of the next switching point and then show that $\xi/\zeta = -\mu/\kappa$ while $(\zeta, \xi) \neq (\kappa, -\mu)$ [1]. Subsequently, integrating the equations for the inter-switching time given in (14), we can also show that $\nu/\lambda = -\xi/\zeta$ and $(\lambda, \nu) \neq (\zeta, -\xi)$ [1].

Alternatively, we present a more elegant proof based on the symmetries of the system. Observe that the transformation $(t, x_1, x_2) \to (-t, x_1, -x_2)$ leaves the system (5) and (6) invariant for constant u. So, starting from (ζ, ξ) and running the system backwards to the next (previous in the forward direction) switching point (κ, μ), the switching time is given by a relation similar to (13), with $x_2/x_1 = -\xi/\zeta$. But this switching time is the same as in the forward direction, where $x_2/x_1 = \mu/\kappa$ in (13). Then, using (13), it is not hard to see that $\xi/\zeta = -\mu/\kappa$. Note that $\zeta = \kappa$ would imply $\xi = -\mu$, i.e. returning to the same point on the x_1-axis with opposite velocity before switching again, which is obviously not time optimal. Thus, it is $\zeta \neq \kappa$ in general so $(\zeta, \xi) \neq (\kappa, -\mu)$.

$\blacksquare$
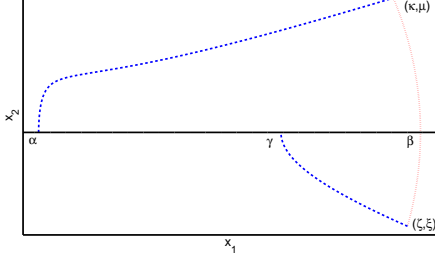
Fig. 3. Blue dashed curves correspond to X-segments, red dotted curves to Y-segments.

In the following proposition we use Lemma 3 to determine the form of the optimal trajectory.

Proposition 4 (Form of the optimal trajectory): The optimal trajectory can have the one-switching form XY or the spiral form $YX\dots YXY$ with an even number of switchings.

Proof: We first show that when the optimal trajectory has more than one switching, it cannot start with an X-segment. For just two switchings, consider the trajectory XYX depicted in Fig. 3, where $\alpha = 1$ (starting point), $(\gamma, 0), \gamma > 1$ is the target point and $(\kappa, \mu), (\zeta, \xi)$ are the switching points. Since both of the switching points belong to the Y-segment passing through $(\beta, 0)$, their coordinates satisfy (12). If we denote by s the common ratio $\mu^2/\kappa^2 = \xi^2/\zeta^2 = s$, then both κ, ζ satisfy the equation

$$(s + u_2)x_1^4 - (u_2\beta^2 + \frac{1}{\beta^2})x_1^2 + 1 = 0,$$

so

$$\kappa^2\zeta^2 = \frac{1}{s + u_2} < 1,$$

since $u_2 \geq 1, s > 0$. But also $\kappa^2\zeta^2 > 1$, since $\kappa^2 > 1$ and $\zeta^2 > \gamma^2 > 1$. Thus this trajectory cannot be optimal.

For more switchings, consider the case shown in Fig 2, where now $\alpha = 1$, and use s to denote the common ratio of the squares of the coordinates at the switching points. If τ is the switching time between (ζ, ξ) and (λ, ν), then from (14) we obtain

$$\frac{s}{u_1} = \frac{\cosh(2\tau\sqrt{u_1}) + 1}{\cosh(2\tau\sqrt{u_1}) - 1} > 1.$$

But $s/u_1 = \mu^2/(u_1\kappa^2)$, and from (11) we find ($\alpha = 1$)

$$\frac{s}{u_1} = \frac{(u_1\kappa^2 + 1)(\kappa^2 - 1)}{u_1\kappa^4} < 1 \Leftrightarrow (u_1 - 1)\kappa^2 > -1,$$

since $u_1 \geq 1$. Thus if the optimal trajectory has more than one switching, it needs to start with a Y-segment.

We next show that the optimal trajectory reaches the target point $(\gamma, 0), \gamma > 1$ with a Y-segment. This is obviously the case for one switching, and also for two switchings since only the YXY trajectory is permitted (the XYX was excluded above). For more than two switchings consider the situation shown in Fig. 3. It is $\mu^2/\kappa^2 = \xi^2/\zeta^2 = s$ and $s > u_1$ since at least one YXY-segment is included in the trajectory. Point (ζ, ξ) belongs to the final X-segment ending to $(\gamma, 0)$, so

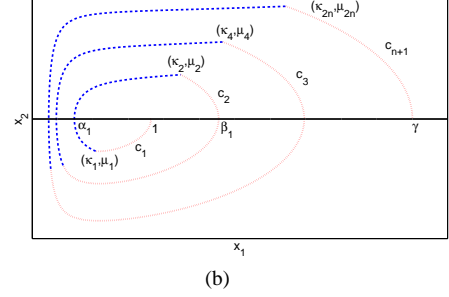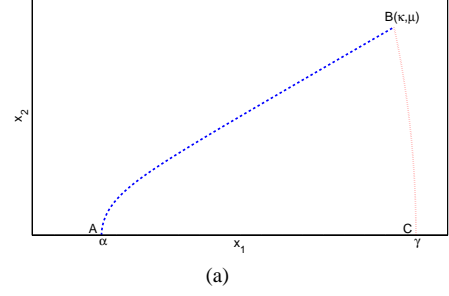$$(s - u_1)\zeta^2 + \frac{1}{\zeta^2} = -u_1\gamma^2 + \frac{1}{\gamma^2}.$$

(a)

(b)

Fig. 4. (a) Trajectory with one switching (zero turns) (b) Trajectory with n turns.

The left hand side is positive, since $s > u_1$, while the right had side is negative, since $\gamma > 1, u_1 \geq 1$. Thus the optimal trajectory reaches the target point with a Y-segment. ∎

Corollary 1: For $|u| \leq 1$ the optimal solution has only one switching.

Proof: For $u = u_2 = 1$ the starting point $(1, 0)$ is an equilibrium point of system (5), (6). So the optimal trajectory cannot start with a Y-segment. The only trajectory thus permitted is XY ∎

From Proposition 4 we see that the optimal trajectory can have aside from the expected one-switching form, shown in Fig. 4(a), the spiral form shown in Fig. 4(b). An intuitive understanding of this latter form can be obtained by viewing system equations (5), (6) as describing the motion of a unit mass particle with position x_1 and velocity x_2. In light of this interpretation we see that along a spiral trajectory the particle, instead of moving directly to the target, goes close to $x_1 = 0$ where there is a strong repulsive potential $(1/x_1^3)$ to acquire speed and reach the target point faster. In the following theorem we calculate the transfer time for the candidate optimal trajectories.

Theorem 2: Starting from $(1, 0)$, the necessary time to reach the target point $(\gamma, 0), \gamma > 1$ with one switching is

$$T_0 = \frac{1}{\sqrt{u_1}} \sinh^{-1}\left(\sqrt{\frac{u_1(\gamma^2 - 1)(u_2\gamma^2 - 1)}{\gamma^2(u_1 + u_2)(u_1 + 1)}}\right)$$
$$+ \frac{1}{\sqrt{u_2}} \sin^{-1}\left(\sqrt{\frac{u_2(\gamma^2 - 1)(u_1\gamma^2 + 1)}{(u_1 + u_2)(u_2\gamma^4 - 1)}}\right). \quad (18)$$

The necessary time to reach the target with n turns ($2n$ switchings) is

$$T_n = T_I + nT_X + (n - 1)T_Y + T_F, \quad (19)$$

where

$$T_I = \frac{1}{2\sqrt{u_2}} \cos^{-1}\left(-\frac{sc_1 + u_2\sqrt{c_1^2 - 4(s+u_2)}}{(s+u_2)\sqrt{c_1^2 - 4u_2}}\right), \quad (20)$$

$$T_F = \frac{1}{2\sqrt{u_2}} \cos^{-1}\left(\frac{-sc_{n+1} + u_2\sqrt{c_{n+1}^2 - 4(s+u_2)}}{(s+u_2)\sqrt{c_{n+1}^2 - 4u_2}}\right), \quad (21)$$

$$T_X = \frac{1}{2\sqrt{u_1}} \cosh^{-1}\left(\frac{s+u_1}{s-u_1}\right), \quad (22)$$

$$T_Y = \frac{1}{2\sqrt{u_2}} \left(2\pi - \cos^{-1}\left(\frac{s-u_2}{s+u_2}\right)\right), \quad (23)$$

$$c_1 = u_2 + 1, \quad (24)$$

$$c_{n+1} = u_2\gamma^2 + \frac{1}{\gamma^2}, \quad (25)$$

and s is the solution of the transcendental equation

$$\frac{c_1 + \sqrt{c_1^2 - 4(s+u_2)}}{c_{n+1} + \sqrt{c_{n+1}^2 - 4(s+u_2)}} = \left(\frac{s-u_1}{s+u_2}\right)^n \quad (26)$$

in the interval $u_1 < s \le (u_2 - 1)^2/4$. The constants c_1 and c_{n+1} characterize the first and the last Y-segments, respectively, of the trajectory. The number of turns satisfies the following inequality

$$n \le \left[\frac{T_0}{T_X(s_+)}\right], \quad (27)$$

where $s_+ = (u_2 - 1)^2/4$ and $[\,]$ denotes the integer part.

Proof: In Fig. 4(a) we show a trajectory with one switching point $B(\kappa, \mu)$. The coordinates of this point satisfy equations (11) and (12) with $\alpha = 1$ and $\beta = \gamma$,

$$\mu_2^2 - u_1\kappa^2 + \frac{1}{\kappa^2} = 1 - u_1,$$

$$\mu^2 + u_2\kappa^2 + \frac{1}{\kappa^2} = u_2\gamma^2 + \frac{1}{\gamma^2},$$

from which we find

$$\kappa^2 = \frac{u_2\gamma^4 + 1 + \gamma^2(u_1 - 1)}{\gamma^2(u_1 + u_2)}.$$

By integrating the equations of motion (5) and (6), we find the necessary time along each segment of the trajectory, AB and BC. The total transfer time is the sum of these times and is given by (18). Next consider the case with n turns and $2n$ switching points (κ_j, μ_j), Fig. 4(b), with constant ratio $\mu_j^2/\kappa_j^2 = s$. The first switching point satisfies the equations

$$\mu_1^2 + u_2\kappa_1^2 + \frac{1}{\kappa_1^2} = c_1, \quad (28)$$

$$\mu_1^2 - u_1\kappa_1^2 + \frac{1}{\kappa_1^2} = c, \quad (29)$$

where c_1 is given by (24) and $c = -u_1\alpha_1^2 + 1/\alpha_1^2$, while the second switching point satisfies

$$\mu_2^2 + u_2\kappa_2^2 + \frac{1}{\kappa_2^2} = c_2, \quad (30)$$

$$\mu_2^2 - u_1\kappa_2^2 + \frac{1}{\kappa_2^2} = c, \quad (31)$$

where $c_2 = u_2\beta_1^2 + 1/\beta_1^2$. The constants c_1 and c_2 characterize the first and second Y-segments of the trajectory, while the constant c characterizes the X-segment joining them. Subtracting (29) from (31) and using Lemma 3 which assures that $\kappa_1 \ne \kappa_2$ (consecutive switching points are not symmetric with respect to x_1-axis) we find that

$$s - u_1 - \frac{1}{\kappa_1^2 \kappa_2^2} = 0. \quad (32)$$

But from (28), (30) and the constant ratio relation we find

$$\kappa_1^2 = \frac{2}{c_1 + \sqrt{c_1^2 - 4(s+u_2)}},$$

$$\kappa_2^2 = \frac{c_2 + \sqrt{c_2^2 - 4(s+u_2)}}{2(s+u_2)},$$

where, while solving the quadratic equations we used the $-$ sign for the first and the $+$ sign for the second switching point. The choice of sign for the first switching point will be justified below, while the choice of sign for consecutive switching points should be alternating to avoid picking the symmetric image of the previous point. Using these relations, (32) takes the form

$$\frac{c_1 + \sqrt{c_1^2 - 4(s+u_2)}}{c_2 + \sqrt{c_2^2 - 4(s+u_2)}} = \frac{s - u_1}{s + u_2}.$$

By repeating the above procedure for all the consecutive pairs of switching points, we find

$$\frac{c_i + \sqrt{c_i^2 - 4(s+u_2)}}{c_{i+1} + \sqrt{c_{i+1}^2 - 4(s+u_2)}} = \frac{s - u_1}{s + u_2}, \ i = 1, 2, \ldots, n.$$

Multiplying the above equations we obtain (26), *one* transcendental equation for the ratio s. If we choose the $+$ sign in the quadratic equation for κ_1^2, we obtain an equation similar to (26) but with inverted left hand side. It is $c_{n+1} > c_1 \Leftrightarrow (\gamma^2 - 1)(u_2\gamma^2 - 1) > 0$ and $c_1, c_{n+1} > 0$, so

$$\frac{c_{n+1} + \sqrt{c_{n+1}^2 - 4(s+u_2)}}{c_1 + \sqrt{c_1^2 - 4(s+u_2)}} > 1 > \left(\frac{s-u_1}{s+u_2}\right)^n,$$

and the corresponding transcendental equation has no solution. Note that the left hand side of (26) is a decreasing function of s while the right hand side is an increasing one, so if a solution exists, it is unique. The ratio is bounded below by the requirement $s/u_1 > 1$ and above by $c_1^2 - 4(s+u_2) \ge 0 \Leftrightarrow s \le s_+ = (u_2 - 1)^2/4$. This is also the maximum value of s on the first Y-segment (28). Once we have calculated this ratio, we can find the time interval between consecutive switchings using (22) for an X-segment and (23) for a Y-segment, relations obtained from Lemma 2 on the inter-switching time. Observe that the times along all intermediate X- (respectively Y-) trajectories are equal. The initial time interval T_I (from the starting point up to the first switching) and the final time interval T_F (from the last switching up to the target point) can be easily calculated and are given in (20) and (21), respectively. The total duration T_n of the trajectory with n turns joining the points $(1, 0)$ and $(\gamma, 0)$ is given by (19). Observe that $T_n(s) > nT_X(s) \ge nT_X(s_+)$,
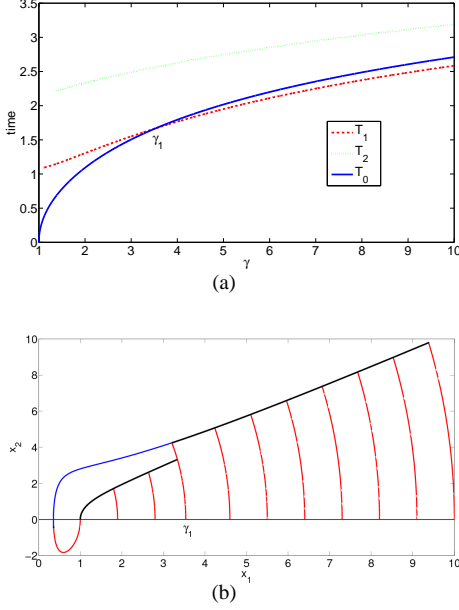
Fig. 5. (a) Transfer times corresponding to zero, one and two turns for $u_1 = 1, u_2 = 8, \gamma \in [1, 10]$. (b) Switching curves (black solid curves) and characteristic optimal trajectories starting from $(1, 0)$.
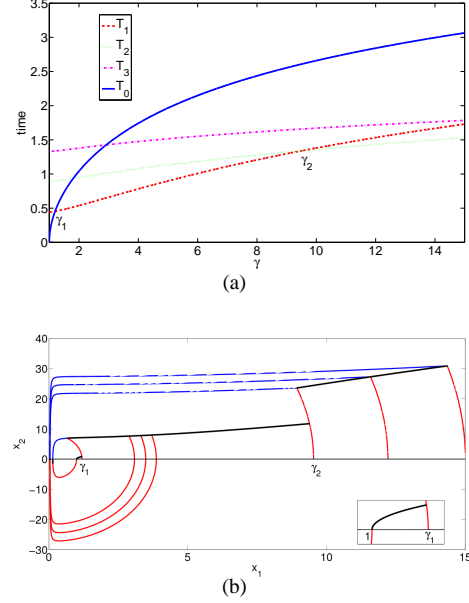

Fig. 6. (a) Transfer times corresponding to zero, one, two and three turns for $u_1 = 1, u_2 = 50, \gamma \in [1, 15]$. (b) Switching curves (black solid curves) and characteristic optimal trajectories starting from $(1, 0)$.

where the last inequality follows from the fact that T_X is a decreasing function of s, see (22). A solution with n turns can be candidate for optimality only if the number of turns is bounded as in (27). Otherwise we have $T_n(s) > T_0$ and the one-switching strategy is faster. ∎

Using Theorem 2 we can find the times T_n for a specific target $(\gamma, 0)$ and compare them to obtain the minimum time.

IV. EXAMPLES

In Fig. 5(a) we plot the times T_0, T_1 and T_2 from Theorem 2, corresponding to zero, one and two turns, for $u_1 = 1, u_2 = 8$ and $\gamma \in [1, 10]$. For $\gamma \leq \gamma_1$ the strategy with zero turns (one switching) is optimal, while for $\gamma \geq \gamma_1$ it is the strategy with one turn (up to the range of γ plotted). The point $(\gamma_1, 0)$ can be reached with both strategies in equal time, that is, it belongs to the cut-locus of these two control sequences from $(1, 0)$. Note that the strategies with one and two turns are feasible after some $\gamma > 1$, where the transcendental equation (26) has a solution. In Fig. 5(b) we plot the switching curves (black solid curves) as well as some characteristic optimal trajectories starting from $(1, 0)$. For $\gamma \leq \gamma_1$ the optimal trajectory starts with an X-segment that coincides with the switching curve (black solid curve) passing from $(1, 0)$. It switches at some point and then travels along a Y-segment (red dotted curve) to meet the x_1-axis. For $\gamma \geq \gamma_1$ the optimal trajectory starts with a Y-segment (red dotted curve passing from $(1, 0)$) and switches at some point in the tiny black area of this curve to an X-segment (blue dashed curve). Then it meets at some point the second switching curve on the upper quadrant and changes to a Y-segment (red dotted curve) that hits the x_1-axis at the target point. Note that the optimal trajectories between the two switchings (blue dashed curves) are very close to the

second switching curve on the upper quadrant and they are not shown entirely.

In Fig. 6(a) we plot the times T_0, T_1, T_2 and T_3 from Theorem 2, corresponding to zero, one, two and three turns, for $u_1 = 1, u_2 = 50$ and $\gamma \in [1, 15]$. Again, for small γ the one-switching strategy is optimal and after some $\gamma = \gamma_1$ the one-turn strategy becomes faster, but there is also a $\gamma = \gamma_2$ beyond which the two-turn strategy is optimal (up to the range of γ plotted). The point $(\gamma_2, 0)$ thus belongs to the cut-locus of the one- and two-turn control sequences from $(1, 0)$ since it can be reached with one or two turns in equal time. In Fig. 6(b) we plot the switching curves (black solid curves) along with some characteristic optimal trajectories starting from $(1, 0)$. For $\gamma \geq \gamma_2$ the optimal trajectory makes an additional turn. This is demonstrated by the three adjacent Y-segments (red dotted curves), which switch close to 0 to the corresponding X-segments (blue dashed curves), on a tiny switching curve which is hardly seen. In turn, these trajectories switch on the third switching curve on the upper quadrant to Y-segments (red dotted curves) that hit the x_1-axis at the target points.

V. CONCLUSION AND FUTURE WORK

In this article we solved a time-optimal control problem related to frictionless atom cooling in harmonic traps. The results presented here can be immediately extended to the fast frictionless expansion of a two-dimensional Bose-Einstein condensate confined in a parabolic trapping potential [28], with possible application in atom interferometry, and even to the implementation of a quantum dynamical microscope, a controlled expansion that allows to scale up an initial many-body state of an ultracold gas by a desired factor while preserving the quantum correlations of the initial state [29].

This work has also been used to show how the third law of classical thermodynamics, known as unattainability principle, emerges from quantum thermodynamics [23]. In a dynamical interpretation, this law states that absolute zero is unattainable, since the cooling rate from a thermal bath with falling temperature declines as well and approaches zero with an appropriate power of the temperature. The heat machine used to demonstrate this is a quantum refrigerator, the quantum analog of the classical Otto cycle, where the working medium is made up of particles in a harmonic (possibly repelling) potential instead of classical particles in a piston. The initial frequency coincides with the maximum allowed frequency as well as the strongest repelling frequency, so $u_1 = u_2 = 1$. From Corollary 1 we see that the minimum time T for the adiabatic-like cooling branch is given by equation (18) in Theorem 2. As the temperature approaches zero, $\omega_T \to 0$ and $\gamma = \sqrt{\omega_0/\omega_T} \to \infty$, so the cooling time approaches infinity logarithmically, $T \sim \ln \gamma$ [22].

REFERENCES

[1] D. Stefanatos, H. Schaettler, and J.-S. Li, "Minimum-time frictionless atom cooling in harmonic traps", *SIAM J. Control Optim.*, vol. 49, pp. 2440-2462, 2011.

[2] H. Mabuchi and N. Khaneja, "Principles and applications of control in quantum systems", *Int. J. Robust Nonlinear Control*, vol. 15, pp. 647–667, 2005.

[3] A. C. Doherty, S. Habib, K. Jacobs, H. Mabuchi, and S. M. Tan, "Quantum feedback control and classical control theory", *Phys. Rev. A*, vol. 62, 012105, 2000.

[4] M. R. James, H. I. Nurdin, and I. R. Petersen, "H^∞ control of linear quantum stochastic systems", *IEEE Trans. Automat. Control*, vol. 53, pp. 1787–1803, 2008.

[5] N. Khaneja, R. Brockett, and S. J. Glaser, "Time optimal control in spin systems", *Phys. Rev. A*, vol. 63, 032308, 2001.

[6] D. D'Alessandro and M. Dahleh, "Optimal control of two-level quantum systems", *IEEE Trans. Automat. Control*, vol. 46, pp. 866–876, 2001.

[7] U. Boscain, G. Charlot, J.-P. Gauthier, S. Guerin, and H.-R. Jauslin, "Optimal control in laser-induced population transfer for two- and three-level quantum systems", *J. Math. Phys.*, vol 43, pp. 2107–2132, 2002.

[8] D. Stefanatos, N. Khaneja, and S. J. Glaser, "Optimal control of coupled spins in the presence of longitudinal and transverse relaxation", *Phys. Rev. A*, vol. 69, 022319, 2004.

[9] B. Bonnard, M. Chyba, and D. Sugny, "Time-minimal control of dissipative two-level quantum systems: The generic case", *IEEE Trans. Automat. Control*, vol. 54, pp. 2598–2610, 2009.

[10] D. Stefanatos and J.-S. Li, "Constrained minimum-energy optimal control of the dissipative Bloch equations", *Systems Control Lett.*, vol. 59, pp. 601–607, 2010.

[11] A. Peirce, M. Dahleh, and H. Rabitz, "Optimal control of quantum mechanical systems: Existence, numerical approximations, and applications", *Phys. Rev. A*, vol. 37, pp. 4950–4964, 1988.

[12] N. Khaneja, T. Reiss, C. Kehlet, T. Schulte-Herbrüggen, and S. J. Glaser, "Optimal control of coupled spin dynamics: Design of NMR pulse sequences by gradient ascent algorithms", *J. Magn. Reson.*, vol. 172, pp. 296–305, 2005.

[13] J.-S. Li, J. Ruths, and D. Stefanatos, "A pseudospectral method for optimal control of open quantum systems", *J. Chem. Phys.*, vol. 131, 164110, 2009.

[14] C. E. Wieman, D. E. Pritchard, and D. J Wineland, "Atom cooling, trapping, and quantum manipulation", *Rev. Mod. Phys.*, vol. 71, pp. S253–S262, 1999.

[15] J. I. Cirac and P. Zoller, "New frontiers in quantum information with atoms and ions", *Physics Today*, vol. 57, pp. 38-44, 2004.

[16] H. R. Lewis and W. B. Riesenfeld, "An exact quantum theory of the time-dependent harmonic oscillator and of a charged particle in a time-dependent electromagnetic field", *J. Math. Phys.*, vol. 10, pp. 1458–1473, 1969.

[17] A. E. Leanhardt, T. A. Pasquini, M. Saba, A. Schirotzek, Y. Shin, D. Kielpinski, D. E. Pritchard, and W. Ketterle, "Adiabatic and evaporative cooling of Bose-Einstein condensates below 500 picokelvin", Science, vol. 301, pp. 1513–1515, 2003.

[18] S. Bize, P. Laurent, M. Abgrall, H. Marion, I. Maksimovic, L. Cacciapuoti, J. Grnert, C. Vian, F. Pereira dos Santos, P. Rosenbusch, P. Lemonde, G. Santarelli, P. Wolf, A. Clairon, A. Luiten, M. Tobar, and C. Salomon, "Cold atom clocks and applications", *J. Phys. B: At. Mol. Opt. Phys.*, vol. 38, pp. S449–S468, 2005.

[19] P. Salamon, K. H. Hoffmann, Y. Rezek, and R. Kosloff, "Maximum work in minimum time from a conservative quantum system", *Phys. Chem. Chem. Phys.*, vol. 11, pp. 1027-1032, 2009.

[20] X. Chen, A. Ruschhaupt, S. Schmidt, A. del Campo, D. Guéry-Odelin, and J. G. Muga, "Fast optimal frictionless atom cooling in harmonic traps: Shortcut to adiabaticity", *Phys. Rev. Lett.*, vol. 104, 063002, 2010.

[21] D. Stefanatos, J. Ruths, and J.-S. Li, "Frictionless atom cooling in harmonic traps: A time-optimal approach", *Phys. Rev. A*, vol. 82, 063422, 2010.

[22] K.-H. Hoffmann, P. Salamon, Y. Rezek, and R. Kosloff, "Time-optimal controls for frictionless cooling in harmonic traps", *Europhys. Lett.*, vol. 96, 60015, 2011.

[23] Y. Rezek, *Heat Machines and Quantum Systems: Towards the Third Law*, PhD Thesis, Hebrew University of Jerusalem; 2011.

[24] E. Merzbacher, *Quantum Mechanics*, John Wiley and Sons, New York; 1998.

[25] L. S. Pontryagin, V. G. Boltyanskii, R. V. Gamkrelidze, and E. F. Mishchenko, *The Mathematical Theory of Optimal Processes*, Interscience Publishers, New York; 1962.

[26] H. J. Sussmann, "The structure of time-optimal trajectories for single-input systems in the plane: The C^∞ nonsingular case", *SIAM J. Control Optim.*, vol. 25, pp. 433–465, 1987.

[27] V. Jurdjevic, *Geometric Control Theory*, Cambridge University Press, Cambridge; 1997.

[28] J. G. Muga, X. Chen, A. Ruschhaupt, and D. Guéry-Odelin, "Frictionless dynamics of Bose-Einstein condensates under fast trap variations", *J. Phys. B: At. Mol. Opt. Phys.*, vol. 42, 241001, 2009.

[29] A. del Campo, "Frictionless quantum quenches in ultracold gases: A quantum dynamical microscope", *Phys. Rev. A*, vol. 84, 031606(R), 2011.